Hindawi
Mathematical Problems in Engineering
Volume 2022, Article ID 2242338, 13 pages
https://doi.org/10.1155/2022/2242338

Research Article

Parameters Optimization-Based Tracking Control for Unmanned Surface Vehicles

Renqiang Wang,[1] **Huaran Yan**,[2] **Qinrong Li**,[3] **Yubo Deng**,[1] **and Yutong Jin**[1]

[1]*Navigation College, Jiangsu Maritime Institute, Nanjing 211170, China*
[2]*Merchant Marine College, Shanghai Maritime University, Shanghai 201306, China*
[3]*Transport Planning and Research Institute, Ministry of Transport of China, Beijing 100028, China*

Correspondence should be addressed to Renqiang Wang; wangrenqiang2009@126.com

Received 8 September 2021; Revised 18 October 2021; Accepted 21 February 2022; Published 18 March 2022

Academic Editor: Haoqian Huang

In this paper, a type of tracking controller on the basis of parameters optimization was proposed for unmanned surface vehicles (USVs). Taking into account the unique nonlinear and large inertia characteristics of USVs, an iterative sliding mode control (ISMC) was adopted to construct the controller including the USVs' main engine speed controller to determine the longitudinal velocity and the steering controller to control the lateral displacement. In designing, the hyperbolic tangent function with the saturation characteristic is introduced to design the output feedback control law of nonlinear iterative sliding mode. Then, the differential evolution algorithm (DEA) is applied to construct the parameters optimization system for acquiring the optimal parameters of the proposed controller, and the control quality with adaptive ability and robustness of the optimized controller is achieved. It is verified by computer experiments that the optimized controller realizes the tracking control for USV under interference; meanwhile, compared with the iterative sliding mode controller, the control performance of the controller is better and the robustness of that is stronger.

1. Introduction

In recent years, the development of information, computers, artificial intelligence, and other technologies has greatly promoted the process of ship intelligence, making it possible to realize unmanned smart ships. Smart ships are the inevitable trend of future ship development and have good application requirements and development prospects. Unmanned surface vessels (USVs) are one of the ways to move towards unmanned ships. Among them, autonomous navigation technology including ship course tracking control and trajectory tracking control is one of the core technologies of unmanned ship motion control and has become a research hotspot in the academic world. The engineering requirements put forward higher requirements for the accuracy of USV control, studying the motion control of underactuated USV having important theoretical significance and practical value. However, the unique underactuated characteristics of the USV and the changeable external environment seriously affect its operating performance.

The application prospect of ships' trajectory tracking control in practical engineering is promoted by increasing of research on trajectory tracking control. The simulation of tracking the preset ships' trajectory on the actual model of 1 : 70 was realized on the basis of the output feedback method proposed by Michiel [1]. Zhao [2] combined sliding mode control and reinforcement learning algorithms and used an adaptive integral sliding mode controller to suppress chattering, but this method can only be used for tensor product models. He [3] combined the robust adaptive learning control method and the sliding mode control method to complete the trajectory tracking and directly used the integral sliding mode surface to suppress chattering. However, the disadvantage of [1–3] is that they are all in the ideal state, i.e., no disturbance or just continuous disturbance. In order

to improve the dynamic disturbance immunity of the control algorithm, the trajectory tracking under the time-varying disturbance was achieved based on the backstepping method proposed by Yang [4]. Besides, the model predictive control was proposed by Annamalai [5] to control the sudden disturbance of the ship, and the effectiveness was verified by simulation experiments.

Sliding mode control method was applied to the tracking control for ships or USVs with the uncertainty. An adaptive terminal sliding mode tracking control with nonsingular integral-type second order was proposed by Saleh Mobayen [6] for dynamic nonlinear system with uncertainties. And the method is applied to the thruster system, so that the chattering of the control output is lower and the amplitude is smaller. The proportional integral derivative (PID) control mode is incorporated into the sliding surface designing, and an adaptive PID-SMC technique is constructed to realize tracking control of UAVs with disturbances [7]. The radial basis function (RBF) neural network [8] online compensation is integrated into the sliding mode control designing, which solves the control input limitation problem of the USV motion system. At the same time, the RBF neural network also reduces the chattering [9] of control system designed by user. Literature [10] uses model predictive control to adapt to the environment online to control the sudden disturbance of the ship, with good results. The application of sliding mode control to ship trajectory tracking has similar research results. The auxiliary compensation system constructed by RBF is directly used to solve the input saturation problem of ship, and the desired effect that control input jumps out of the saturation limit area was achieved [11]. In literature [12], in view of the uncertainty of model parameters and the time-varying interference of wind, wave, and current, a sliding mode control method was adopted to construct the controller which tracks the virtual ship's reference trajectory. In order to obtain a better control effect, the literature [13] used coordinate changes to transform the system into a chain system, designed an exponential control law, designed a sliding mode controller based on a nonlinear model, and achieved good results in the simulation process. In literature [14], a method to robust controllers with model uncertainty and different types of disturbances was proposed by using sliding mode control technology, so that the scheme of waypoint tracking for underactuated autonomous underwater vehicles was developed.

Regarding engineering requirements, the output and velocity constraints of USVs should be considered to improve safety for USVs. In literature [15], by introducing a barrier Lyapunov function into the line-of-sight guidance, the specific transient tracking performance in terms of position error is guaranteed. A novel constrained yaw rate controller is proposed to ensure time-varying yaw rate constraint satisfaction, in which the yaw rate barrier is required to vary with the speed of the hovercraft. The neuroadaptive control for complicated underactuated systems with simultaneous output and velocity constraints [16] was proposed by Yang Tong. Different output constraint-related auxiliary functions are constructed in the Lyapunov function candidate to generate nonlinear displacement/angle-limited terms to control all state variables. Then, the elaborately designed velocity constraint-related terms are directly introduced into the presented controller, so that both actuated and unactuated velocity constraints are ensured.

On the mathematical model of dynamic motion of USVs, based on the response model and the Fossen model, there is a big gap between the control inputs including control forces and torques, obtained by the above control method and the actual propulsion input of USVs. Especially for the underactuated USVs with single propeller and single rudder, the control inputs should be obtained in the form of rudder angle and main engine speed [17]. For this, the control inputs in the form of rudder angle and main engine speed were achieved for trajectory tracking control of underactuated USVs [18], under the nonlinear separation model proposed by mathematical model group (MMG) [19]. Similarly, Jia Heming [20] adopted nonlinear iterative sliding mode methods to control the course and track tracking of surface ships and unmanned underwater vehicles, respectively, and achieved good control effects. On the one hand, this method avoids the linearity of the model; on the other hand, it also avoids the uncertainty in USVs' model and uncertain interference items. However, the parameters of the controller are fixed and make the controller not adaptive. The adaptive recursive sliding mode control strategy [21] with minimum parameter was proposed for nonlinear system with time varying, which expands the limited output range.

Nowadays, intelligent control technology is developing rapidly. Moreover, some intelligent control methods, such as neural network [20] and fuzzy algorithm [22], have been used in the design of ship motion tracking control system. In literature [22], Shen proposed a fuzzy and shaped sliding mode flight control method with interesting brain evaluation. The mathematical model of the "Wenzhuhai" bulk carrier was used for control simulation. The results proved that the designed control performance is good and has strong robustness. In literature [23], Zhao Shunli proposed an adaptive sliding mode control method with dynamic surface based on neural network, and simulations show that the ship can quickly stabilize on a certain specified heading. In literature [24], Wang Hao proposed a cooperative path tracking algorithm with dynamic surface based on neural network, which realizes path tracking under interference conditions. In literature [25], Shen Zhipeng introduced a fuzzy system to optimize the predictable sliding mode parameters, designed a flight control that mimics the sliding mode control with sail navigation aids, and achieved good control effects. The particle swarm algorithm (PSA) with swarm optimization performance was used to optimize multiparameters in the iterative sliding mode control of underactuated ships, and the precise control of trajectory tracking is realized [26]. In literature [27], the adaptive sliding mode control with RBF neural network optimized by improved genetic optimization algorithm was designed for ships' heading tracking control, and computer experiments verified the method is effective for steering system. In literature [28], the ship heading control system is designed by

using the adaptive sliding mode control method combined with RBF neural network, which effectively solves the fast heading tracking under the condition of limited control input. It is concluded that in the sliding mode control, the control parameters have a significant effect on the adaptability and robustness of the controller, and the use of intelligent methods to optimize the parameters of the controller can make the control system achieve better accuracy. In addition, as far as the current intelligent optimization algorithm is concerned, under the same circumstances, the differential evolution algorithm (DEA) [29] has been proven to be the fastest evolutionary algorithm compared with genetic algorithm (GA) [30] and particle swarm algorithm (PSA) [26].

Inspired by observations, a type of tracking controller on the basis of parameters optimization was proposed for unmanned surface vehicles (USVs) in paper. Taking into account the unique nonlinear and large inertia characteristics of USVs, an iterative sliding mode control (ISMC) was adopted to construct the controller including the USVs' main engine speed controller to determine the longitudinal velocity and the steering system controller to control the lateral displacement. In designing, the hyperbolic tangent function with the saturation characteristic is introduced to design the nonlinear iterative sliding mode output feedback control law. Then, the differential evolution algorithm (DEA) is applied to construct the parameters optimization system for acquiring the optimal parameters of the proposed controller. With a certain type of USV model, it is obtained by computer experiments that the optimized controller proposed in paper realizes the tracking control for USV under interference; meanwhile, compared with the iterative sliding mode controller, its control performance is better, the control chattering is smaller, and the robustness is stronger.

The merit of the paper is to optimize the previous tracking controller. Specifically, it includes (1) introducing the hyperbolic tangent function with saturation characteristics into the iterative sliding mode design. On the one hand, it can effectively overcome the chattering problem of the control input objectively existing in the sliding mode control design, and, on the other hand, it can also effectively avoid the hassle of getting control inputs into saturation. (2) Using the differential evolution algorithm (DEA) with swarm optimization performance to optimize various control parameters in the iterative sliding mode control design online, the optimization coupling problem of multiple parameters is solved at one time, and the tedious process of repeated trial and error is avoided. It greatly improves the adaptive ability and robustness of the system and conforms to the design and development concept of unmanned boats.

At the same time, it is necessary to solve the speed limitation problem of USV trajectory tracking control. In response to this problem, this paper designs an iterative sliding mode control algorithm based on the speed model of the diesel engine for USV and then guarantees that the speed of the USV meets the set speed range.

2. Problem Description

For the USV equipped with one propeller and one rudder, the driving sources to realize trajectory tracking control are rudder angle and main engine speed, while the driving sources of Fossen model [31] for trajectory tracking control are forces and torques. The MMG model overcomes this shortcoming. So, this paper adopts the MMG model [20, 21] to design the trajectory tracking controller for USVs. The MMG model is expressed as

$$\begin{cases} \dot{u} = \dfrac{\left[\begin{array}{l} X_H + X_P + X_R + X_{\text{wind}} + \\ X_{\text{wave}} + \left(m + m_y\right) vr \end{array}\right]}{\left(m + m_x\right)} \\ \dot{v} = \dfrac{\left[\begin{array}{l} Y_H + Y_P + Y_R + Y_{\text{wind}} + \\ Y_{\text{wave}} - \left(m + m_x\right) ur \end{array}\right]}{\left(m + m_y\right)} \\ \dot{r} = \dfrac{\left[N_H + N_P + N_R + N_{\text{wind}} + N_{\text{wave}}\right]}{\left(I_z + J_z\right)} \\ \dot{x} = u\cos(\varphi) - v\sin(\varphi) + u_c\cos\left(\varphi_c\right) \\ \dot{y} = v\cos(\varphi) + u\sin(\varphi) + u_c\sin\left(\varphi_c\right) \\ \dot{\varphi} = r \end{cases}, \quad (1)$$

where X_H, Y_H, and N_H represent longitudinal force, lateral force, and rotational moment, respectively; X_P, Y_P, and N_P represent the longitudinal force, lateral force, and rotational moment of propeller, respectively; X_R, Y_R, and N_R stand for longitudinal force, lateral force, and rotational moment of rudder, respectively; X_{wind}, Y_{wind}, and N_{wind} represent longitudinal force, lateral force, and rotational moment, respectively; X_{wave}, Y_{wave}, and N_{wave} represent longitudinal force, lateral force, and rotational moment, respectively; m represents USV's mass; m_x and m_y represent additional USV's mass in the longitudinal and transverse directions, respectively; I_z and J_z represent the moment of inertia of the USV, respectively; u stands for USV's longitudinal speed; u_c stands for current speed; v stands for USV's lateral speed; r stands for rotation speed; x and y stand for USV's longitudinal and lateral position; φ stands for USV's heading; and φ_c stands for current direction.

Figure 1 is a schematic diagram of the tracking deviation of the USV trajectory. $O(x_d, y_d)$ is the coordinate of the USV's actual trajectory; $G(x, y)$ is the coordinate of the USV's current trajectory. The distance between these two points is ρ_D. ψ_r is the expected USV's heading and ψ is the USV's heading. x_e and y_e stand for the deviation of longitudinal and lateral of trajectory.

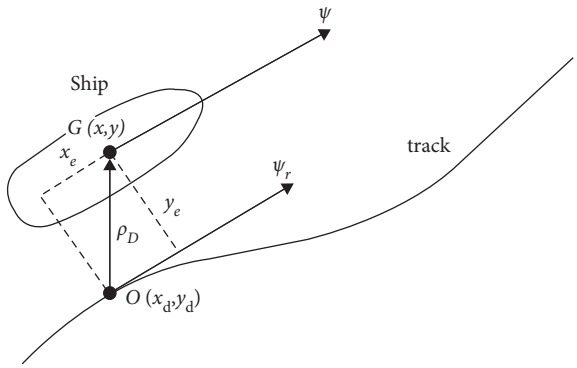

Figure 1: Trajectory tracking diagram for ships.

The expected point of the trajectory points to the actual point and the direction angle is θ_r. So, (2) is obtained from Figure 1.

$$\begin{cases} \psi_r = \arctan\left(\dfrac{\dot{y}_d}{\dot{x}_d}\right) \\ \theta_r = \arctan\left(\dfrac{y - y_d}{x - x_d}\right) \\ \rho_D = \sqrt{(y - y_d)^2 + (x - x_d)^2}\,. \\ x_e = \rho_D \cdot \cos(\theta_r - \psi_r) \\ y_e = \rho_D \cdot \sin(\theta_r - \psi_r) \\ \psi_e = \psi - \psi_r \end{cases} \tag{2}$$

In the actual maneuvering process, according to the characteristics of USV navigation, its speed (including longitudinal and lateral speed), acceleration, and external disturbances are usually smooth and bounded; the longitudinal velocity is greater than the flow velocity, and both are much greater than the lateral velocity; that is, $u > |u_c|?|v|$.

In order to make the track deviation $y_e \longrightarrow 0$, parameters optimization based tracking control for USVs is designed.

3. Design Tracking Controller of USV Motion

3.1. Theorem. In order to facilitate the design of the controller, the theorem is described as follows:

Consider a first-order nonlinear state space model,

$$y = f(x, u, t). \tag{3}$$

where x is the state variable, u is the input, and y is the output.

In order to facilitate the subsequent iterative sliding mode design and solution, the total assumptions need to be considered in the process of designing the USV trajectory controller in this paper.

Assumptions 1 (see [32]).

(1) $f(x, u, t)$ in (3) is a continuous differentiable function.

(2) The gain of the control input is unknown, and it is assumed that $\partial f/\partial u > 0$.

Theorem 1. *The hyperbolic tangent function with saturation characteristic is adopted to construct the nonlinear feedback control law of iterative sliding mode.*

$$\dot{u} = -k_p y - \varepsilon \tanh(y), \tag{4}$$

where $k_p > 0$ *and* $\varepsilon > 0$.

The state function is defined as $\dot{x} = g(u)$, and $g(u)$ represents continuous function with boundness. The uniform asymptotic stabilization of system (3) can be guaranteed under the control law (4).

Proof. First, (5) is derived by taking the derivative of (4).

$$\dot{y} = \frac{\partial f}{\partial x}\dot{x} + \frac{\partial f}{\partial u}\dot{u}. \tag{5}$$

The Lyapunov function is constructed as follows:

$$V(y) = \frac{1}{2}y^2. \tag{6}$$

Then, (6) is referred by taking the derivative of

$$\begin{aligned} \dot{V}(y) = \frac{1}{2}y^2 &= y\dot{y} = y\left(\frac{\partial f}{\partial x}\dot{x} + \frac{\partial f}{\partial u}\dot{u}\right) \\ &= \frac{\partial f}{\partial x}g(u)y + \frac{\partial f}{\partial u}\left[-k_p y - \varepsilon \tanh(y)\right]y \\ &= \left\{\frac{\partial f}{\partial u}\left[-k_p y - \varepsilon \tanh(y)\right] + \frac{\partial f}{\partial x}g(u)\right\}y \\ &\le -\left\{\frac{\partial f}{\partial u}\left[k_p|y| + \varepsilon|\tanh(y)|\right] - \frac{\partial f}{\partial x}g(u)\right\}|y|. \end{aligned} \tag{7}$$

Further, considering $\partial f/\partial u > 0$, the following inequality is obtained with constants k_p and ε.

$$\frac{\partial f}{\partial u}\left[k_p|y| + \varepsilon|\tanh(y)|\right] - \frac{\partial f}{\partial x}g(u) > 0. \tag{8}$$

Furthermore, the following results can be obtained.

$$\dot{V}(y) < 0/. \tag{9}$$

Therefore, the theorem is proved under the assumptions mentioned above. □

3.2. Design ISMC Controller. According to the conceptual analysis of exponential reaching law, the gain term of the sliding mode surface function is to adjust the rise time, and its value is as large as possible; the gain term of the hyperbolic tangent function is used to adjust switching

amplitude, and its value should be as small as possible to weaken the degree of switching. The hyperbolic tangent function is used instead of the sign function to further weaken the system chattering caused by sliding mode surface switching. The gain term of the variable in the hyperbolic tangent function can adjust the amplitude, which promotes the smooth function and weakens the switching.

The lateral component of the ship's trajectory is realized by manipulating the rudder angle. The steering effect produced by steering is restricted by the ship's longitudinal speed. At the same time, the longitudinal component of the ship's trajectory is realized by manipulating the speed of the main engine. Therefore, in order to achieve trajectory tracking control, it is necessary to complete the lateral deviation control and the longitudinal deviation control at the same time.

3.2.1. Design of Iterative Sliding Mode Controller for Longitudinal Deviation. The longitudinal deviation x_e is controlled by changing the speed n of diesel engine, and the feedback control of nonlinear iterative sliding mode is designed as follows:

$$\begin{cases} \sigma_{11}(x_e) = k_{11}\tanh(k_{12}x_e) + \dot{x}_e, \\ \sigma_{12}(\sigma_{11}) = k_{13}\tanh(k_{14}\sigma_{11}) + \dot{\sigma}_{11}, \\ \dot{n}(\sigma_{12}) = -k_{15}\sigma_{12} - k_{16}\tanh(\sigma_{12}), \end{cases} \tag{10}$$

where $\tanh(x)$ is strictly bounded; k_{11}, k_{12}, k_{13}, k_{14}, k_{15}, and k_{16} are design parameters.

It is obtained by (10) that when $\sigma_{12} \longrightarrow 0$, there are $\sigma_{11} \longrightarrow 0$ and $x_e \longrightarrow 0$. So, the control goal becomes a stabilization control problem of σ_{12}.

After expanding σ_{12} in (10), it can be referred that

$$\begin{aligned} \sigma_{12}(\sigma_{11}) &= k_{13}\tanh(k_{13}\sigma_{11}) + k_{11}\frac{d}{dt}\tanh(k_{12}x_e) + \dot{x}_e \\ &= k_{13}\tanh(k_{13}\sigma_{11}) + k_{11}k_{12}\frac{\dot{x}_e}{\cosh^2(k_{12}x_e)} + \dot{x}_e. \end{aligned} \tag{11}$$

Considering the system model in (2), ignoring variables that have nothing to do with the speed, it is obtained that

$$\frac{\partial\sigma_{12}}{\partial n} = \frac{\partial\ddot{x}_e}{\partial n} = \frac{\partial}{\partial n}(\dot{u}\cos\psi_e - \dot{v}\sin\psi_e). \tag{12}$$

When the actual ship is navigating normally, the lateral thrust generated by the propeller can be ignored (except for low-speed reverse). Therefore, (12) can be approximated as

$$\frac{\partial\sigma_{12}}{\partial n} \approx \frac{\partial}{\partial n}(\dot{u}\cos\psi_e) = \frac{\partial \mathrm{X}_P}{\partial n}\cos\psi_e/(m + m_x). \tag{13}$$

The deviation between the heading and the track direction when USV is in normal navigating is generally no more than 90° and the relationship between propeller thrust and speed is strictly monotonic. Therefore, it can be inferred that

$$\frac{\partial\sigma_{12}}{\partial n} > 0. \tag{14}$$

According to (14), it can be seen that since the hyperbolic tangent and hyperbolic cotangent functions are strictly bounded, the design trajectory is sufficiently smooth; if the system is controllable, k_{11}, k_{12}, k_{13}, $k_{14} \in \mathrm{R}$ and ideal speed $n^*(t) \in [-n_{\max}, n_{\max}]$ exist to guarantee $\sigma_{12} \longrightarrow 0$.

According to the theorem, when the system and external interference are sufficiently smooth, the sliding mode surface feedback control law $\dot{n}(\sigma_{12}) = -k_{15}\sigma_{12} - k_{16}\tanh(\sigma_{12})$ can make σ_{12} asymptotically stable. Therefore, the stability of the longitudinal trajectory tracking error x_e is proved, that is, the deviation converges.

3.2.2. Design of Iterative Sliding Mode Controller for Lateral Deviation. In order to construct the first-order function between sliding mode surface and rudder angle δ, a fourth-order nonlinear iterative sliding mode is designed, which is specifically divided into the following steps.

The first step is to design the nonlinear sliding mode of the track deviation as

$$\sigma_{21}(y_e) = k_{21}\tanh(k_{20}y_e) + \dot{y}_e, \tag{15}$$

where $k_{20} \sim k_{21} \in R^+$.

It is obtained that when $\sigma_{21} \longrightarrow 0$, $\dot{y}_e \longrightarrow -k_{21}\tanh(k_0 y_e)$. Therefore, the control of tracking is transformed into the control of σ_{21}.

In the second step, considering the large inertia characteristics of the ship, in order to prevent excessive turn rate, the following sliding mode with integral is designed:

$$\sigma_{22}(\sigma_{21}, \varphi_e) = \psi_e + k_{22}\int \tanh(\sigma_{21})dt\ , \tag{16}$$

where $k_{22} \in R^+$.

Obviously, when $\sigma_{22} \longrightarrow 0$, $\psi_e \longrightarrow -k_{22}\int \tanh(\sigma_{21})dt$ and $\dot{\psi}_e \longrightarrow -k_{22}\tanh(\sigma_{21})$.

Considering that the longitudinal and lateral components of the rudder force are much smaller than the torque and that $u \gg |v|$, it is proved that when $\sigma_{22} \longrightarrow 0$, $\sigma_{21} \longrightarrow 0$ [19]. So, the control of tracking is transformed into the control of σ_{22}.

In the third step, combined with the strictly bounded characteristics of the hyperbolic tangent function, the following sliding mode is designed in order to construct the control rudder angle δ,

$$\begin{cases} \sigma_{23}(\sigma_{22}) = k_{23}\tanh(\sigma_{22}) + \dot{\sigma}_{22} \\ \sigma_{24}(\sigma_{23}) = k_{24}\tanh(\sigma_{23}) + \dot{\sigma}_{23} \end{cases}, \tag{17}$$

where $k_{23} \sim k_{24} \in R^+$.

According to the relationship between the sliding surfaces in (17), the control goal is further transformed from σ_{22} to σ_{24}.

Next, deriving the monotonic function between σ_{24} and δ, the theorem is used to design the feedback control law.

Equation (18) is obtained by expanding σ_{21}.

$$\sigma_{21} = k_{21}\tanh(k_{20}y_e) + v\cos(\psi_e) + u\sin(\psi_e) + u_c\sin(\psi_c), \tag{18}$$

σ_{21} is revisited as the output y of system (3), and σ_{21} is subjected to ψ_e. So, ψ_e is regarded as u in (4).

Further, it is referred that

$$\frac{\partial \sigma_{21}}{\partial \varphi_e} = u\cos(\psi_e) - v\sin(\psi_e). \tag{19}$$

The deviation between the heading and the track direction when USV is in normal navigating is generally no more than 90°. So, $\cos(\psi_e) > 0$, $\sin(\psi_e) > 0$. Furthermore, $u?|v|$. Thus, $\partial\sigma_{21}/\partial\varphi_e > 0$.

Therefore, u is designed as

$$\dot{u} = \dot{\psi}_e = -k_{22}\tanh(\sigma_1). \tag{20}$$

According to the theorem, $\partial\sigma_{21}/\partial\varphi_e > 0$ in (19) achieves asymptotic stability, and $\sigma_{21} \longrightarrow 0$. Thence, y_e is asymptotically stable, too.

Next, $\sigma_{24} \longrightarrow 0$ is realized by a type of control law which is constructed as (21) so that y_e is guaranteed to converge stably.

$$\dot{\delta} = -k_{25}\sigma_{24} - \varepsilon\tanh(\sigma_{24}). \tag{21}$$

where $k_{25} \in R^+$, $\varepsilon \in R^+$.

Equation (22) is acquired by expanding σ_{24}.

$$\begin{aligned}\sigma_{24}(\sigma_{23}) = {} & k_{24}\tan(\sigma_{23}) + k_{23}\frac{[r + k_{22}\tanh(\sigma_{21})]}{[\cosh(\sigma_{22})]^2} + \\ & k_{22}\left\{k_{20}k_{21}\dot{y}_e/[\cosh(k_{20}y_e)]^2 + \ddot{y}_e\right\}/[\cosh(\sigma_{21})]^2 + \\ & \frac{(N_H + N_P + N_R + N_{wind} + N_{wave})}{(I_z + J_z)}.\end{aligned} \tag{22}$$

It is considered that, in (22), N_R, X_R, and Y_R are related to δ, so

$$\begin{aligned}\frac{\partial\sigma_{24}}{\partial\delta} &= \frac{\partial}{\partial\delta}N_R/(I_z + J_z) + \frac{\partial}{\partial\delta}\left\{k_{22}\ddot{y}_e/[\cosh(\sigma_{21})]^2\right\} \\ &= \frac{\partial}{\partial\delta}N_R/(I_z + J_z) \\ &\quad + k_{22}\frac{\partial X_R}{\partial\delta}[\sin(\psi)/(m + m_x)]/[\cosh(\sigma_{21})]^2 \\ &\quad + k_{22}\frac{\partial Y_R}{\partial\delta}\left[\cos(\psi)/\left(m + m_y\right)\right]/[\cosh(\sigma_{21})]^2.\end{aligned} \tag{23}$$

where the calculation of N_R is shown in the following:

$$N_R = (x_R + a_H x_H)F_N\cos\delta, \tag{24}$$

where F_R is the rudder force and $F_R > 0$, x_R is the longitudinal coordinate of the lateral point of action on the rudder, a_H is correction factor, and x_H is the distance from the lateral force to the center of gravity; moreover, x_R, a_H, and x_H are all scalars; δ is the rudder angle of the rudder, and $\cos\delta > 0$ while $\delta \in (-35°, 35°)$.

So, $\partial N_R/\partial\delta > 0$ is established.

Considering the actual steering, X_R and Y_R are all smaller than N_R. With the boundedness of trigonometric function and hyperbolic trigonometric functions, (25) holds under k_{22}.

$$\frac{\partial\sigma_{24}}{\partial\delta} > 0. \tag{25}$$

Forasmuch, from (21), (25), and the theorem, σ_{24} converges to zero asymptotically and y_e shows asymptotic convergence too. Therefore, through the design of the abovementioned control system, the tracking of the planned path of the USV is realized.

3.3. Parameters Optimization Based on DEA. It can be known from the USV's mathematical model of maneuvering motion that the USV's roll and external disturbances will cause frequent chattering of the maneuvering control system. Therefore, the design parameters of the controller must be dynamically adjusted to weaken and overcome this chattering.

To enhance the effectiveness and service life of control system, the parameters ($k_{11} \sim k_{16}, k_{20} \sim k_{25}$) of the designed controller are optimized based on DEA, and the adaptive ability and robustness of the system are improved together. Next, an online optimization system is designed based on DEA as in Figure 2, which is integrated into the trajectory tracking control system designed with ISMC method for USV.

It is known that solving the optimization problem based on DEA is to determine the final optimal gene combination by solving the extreme value of the evaluation index, which is the optimal control parameter combination. Combining with the optimization system design idea of Figure 2, the evaluation index function is constructed:

$$\begin{cases} J = \dfrac{1}{N}\displaystyle\sum_{n=1}^{N}\left(\lambda_1 \cdot y_e^2 + \lambda_2 \cdot \psi_e^2 + \lambda_3 \cdot \widetilde{\delta}^2\right), \\ |y_e| \le D, \end{cases} \tag{26}$$

where J is evaluation index function, y_e is trajectory tracking deviation, ψ_e is heading deviation, $\widetilde{\delta}$ is rudder angle chattering, N is the total number of iteration, and $\lambda_1 \sim \lambda_3$ stand for coefficients. Simultaneously, the sizes of $\lambda_1 \sim \lambda_3$ are set generally on the basis of environmental conditions.

$\widetilde{\delta}$ in (26) is calculated [21] by

$$\widetilde{\delta} = \frac{M - \overline{M}}{\overline{M}}, \tag{27}$$

where $\overline{M}$ is the preset value of rudder angle. M is the cumulative sum of the absolute values through n iterations. If M increases, $\widetilde{\delta}$ increases; conversely, if M decreases, $\widetilde{\delta}$ decreases.

M in (27) is calculated by

$$M(t) = \sum_{t=0}^{n}\rho_k(l)|\delta(t - lT) - \delta[t - (l-1)T]|, \tag{28}$$

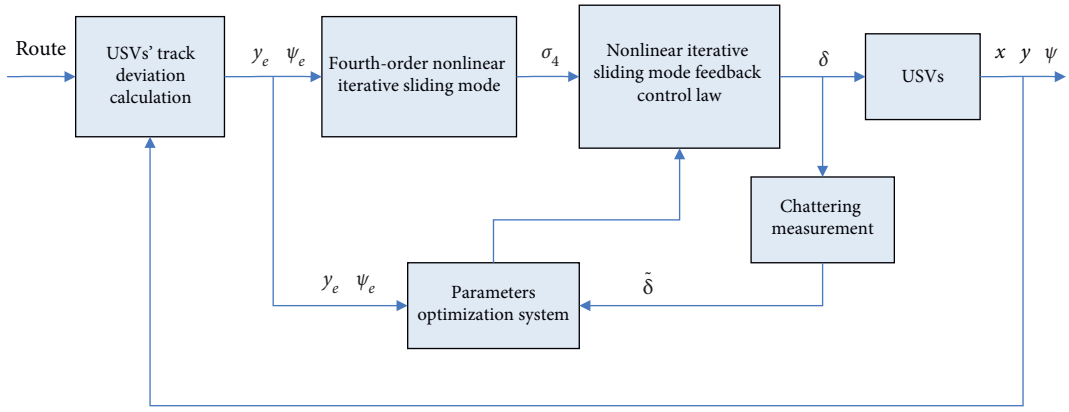

Figure 2: The optimization trajectory tracking control system for USVs.

where T is simulation period, $\delta(t - lT)$ and $\delta[t - (l-1)T]$ are the rudder angle values of different periods, n is the number of accumulation, and $\rho_k(l)$ is defined as

$$\rho_k(l) = \begin{cases} 0, \{\delta_k(lT) - \delta_k[(l-1)T]\} \cdot \{\delta_k[(l-1)T] - \delta_k[(l-2)T]\} \geq 0, \\ 1, \{\delta_k(lT) - \delta_k[(l-1)T]\} \cdot \{\delta_k[(l-1)T] - \delta_k[(l-2)T]\} < 0, \end{cases} \tag{29}$$

If chattering occurs, the trend of the output will change together. The chattering will be acquired in the last cycle by (28).

The process of optimizing the parameters $(k_{11} \sim k_{16}, k_{20} \sim k_{25})$ of the designed controller is shown in Figure 3. The optimized architecture consists of two parts, DEA module and Simulink module. The two parts interact through individual genes (parameters of ISMC controller) and evaluation index function J. Among them, the DEA module assigns parameters to individuals by receiving evaluation indicators; the Simulink module solves the evaluation indicators based on the USB motion model via acquiring the individuals of DEA corresponding to the parameters. The end point of the optimization process is to obtain the smallest evaluation index function.

The solution process of Simulink module can be found in this section, which is the design unit of the control system, and the solution process of the DEA module is as follows.

Step 1. The gene population representing the design parameters of the controller is initialized, and an initial genetic individual $x_i(0)$ is randomly generated.

$$x_{i,0}(0) = rand(i)\left(x^U - x^L\right) + x^L, \tag{30}$$

where $\overset{U}{x}$ and $\overset{L}{x}$ represent the upper and lower limits of the individual; rand(i) is $[0, 1]$.

Step 2. The initial gene population is assigned to parameters $(k_{11} \sim k_{16}, k_{20} \sim k_{25})$ which are transmitted to the Simulink module for performing the track tracking operation. Then, J is calculated and the termination condition is judged. If it is met, end; otherwise, go to Step 3.

Step 3. Mutation Operation. Three individuals ($x_{p_1,j}$, $x_{p_2,j}$, and $x_{p_3,j}$) are selected randomly, which are different from $x_{i,j}$ in j-th generation population, to perform mutation operation for generating a variant gene individual $h_{i,j}(t+1)$.

$$h_{i,j}(t+1) = x_{p_1,j}(t) + F\left(x_{p_2,j}(t) - x_{p_3,j}(t)\right), \tag{31}$$

where $p_1 \sim p_3$ are numbers, $i \neq p_1 \neq p_2 \neq p_3$; G is evolutionary algebra, $j < G$; $F(\cdot)$ is a factor.

Step 4. Cross Operation. To enhance diversity of gene population, new individual $v_i(t+1)$ with variant individual $h_{i,j}(t+1)$ and evolution individual $x_{i,j}(t)$ is generated.

$$v_{i,j}(t+1) = \begin{cases} h_{i,j}(t+1), & r \text{ and } (i) \leq CR, \\ x_{i,j}(t), & r \text{ and } (i) > CR, \end{cases} \tag{32}$$

where CR is probability, and $CR \in [0, 1]$.

Step 5. Next-generation population individuals are generated on the basis of the greedy strategy. $x_i(t+1)$ is chosen by $f(\cdot)$, and next generation particles are generated; then, return to Step 2, and the mentioned-above evolution operation is repeated until G reaches the maximum evolution algebra.

$$x_i(t+1) = \begin{cases} v_i(t+1), f[v_i(t+1)] \leq f[x_i(t)] \\ x_i(t), f[v_i(t+1)] > f[x_i(t)] \end{cases}, \tag{33}$$

where $f(\cdot) = 1/J + 1$.

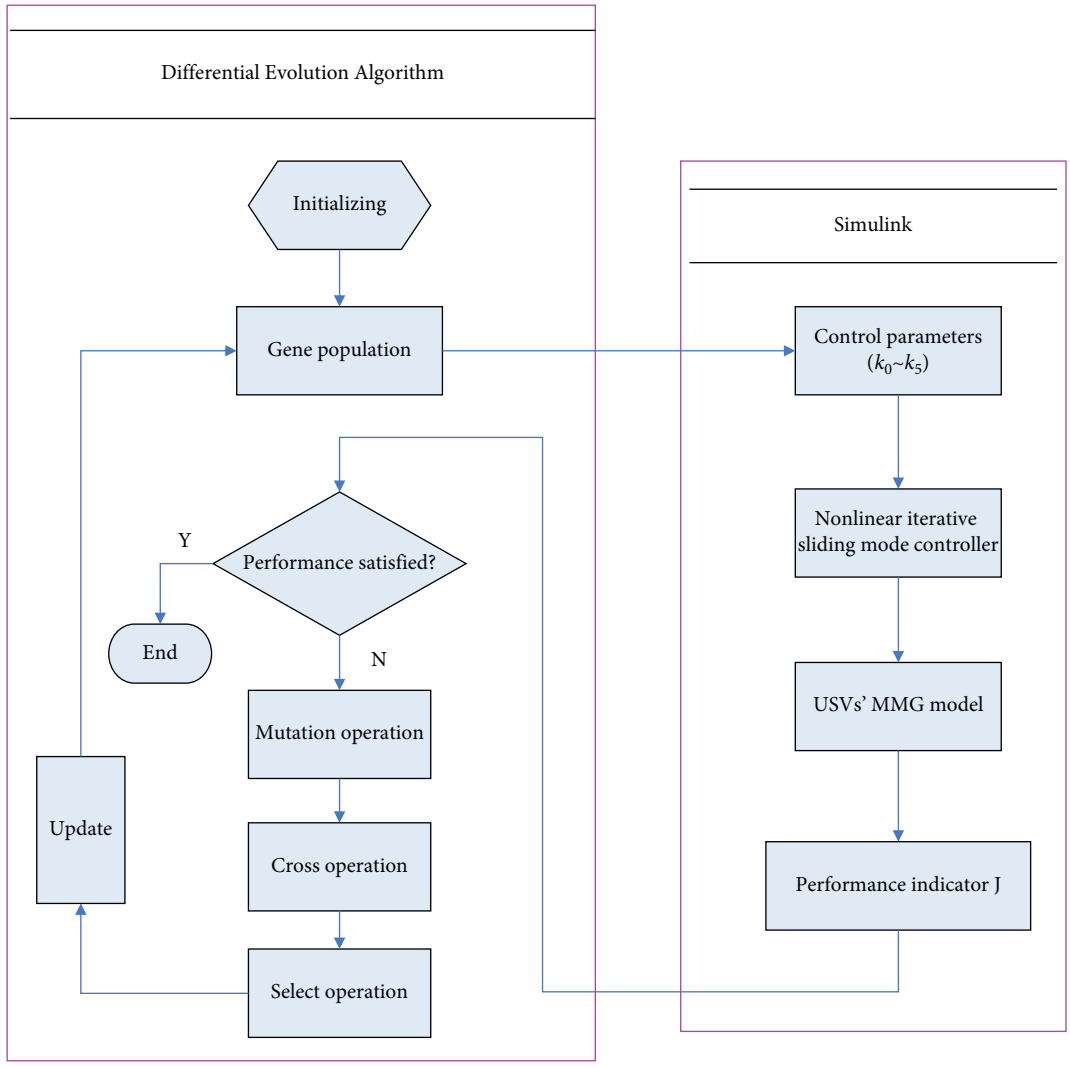

Figure 3: Optimization process of control parameters.

4. Computer Simulation Experiment and Analysis

The USV model in [25] is applied to the computer simulation experiment of trajectory tracking control to verify the adaptive and robust performance of the designed controller. In computer experiment, initial position is (0, 0), speed of engine is 60 RPM, and speed is 15 knots. The center of the planned circular path to be tracked is (2000, 2000) and the radius is 2000 m; wind speed is 10 m/s and direction is 110°; current speed is 1.5 m/s and direction is 110°; wave height is 2 m and the encounter frequency is 0.5 Hz. Since the heading and speed of the USV change at any time, the vector relationship between the USV and the external disturbances also changes at any time. Therefore, the entire test can reflect the adaptability and robustness of the USV under the continuous change of external disturbances.

During the USV's circular trajectory tracking process, the ISMC controller and the DEA-optimized ISMC controller are simultaneously simulated for trajectory tracking. $\varepsilon = 0.001$, $\overline{M} = 0.1$. $k_{11} \sim k_{16}$ of ISMC controller are artificially preset as 10, 5, 15, 8, 26, and 5, and $k_{20} \sim k_{25}$ of the ISMC controller are artificially preset as 17, 8, 7, 5, 16, and 5. $k_{11} \sim k_{16}, k_{20} \sim k_{25}$ of the DEA-optimized ISMC controller are obtained through the online optimization system, and $G = 50$, $CR = 0.75$, and $F = 0.25$ of DEA.

According to the above parameters settings, the two methods are simulated and compared; the description is the part of computer simulation results and analysis in next. First, the evaluation index function curve demonstrating the evolution process is shown in Figure 4. Second, the comparative experiments are shown in Figures 5–12.

It is acquired from the trajectory tracking curve diagram of Figure 5 and the variation curves of the lateral deviation y_e and the longitudinal deviation x_e shown in Figures 6 and 7 that both control methods can completely track the target trajectory. In Figure 6, the lateral deviation of the trajectory tracking control of the DEA-optimized ISMC controller is less than 40m, while the maximum position deviation of the trajectory tracking control of the ISMC controller is 188m, which is about 4.5 times of the former. In Figure 7, the longitudinal deviation of the trajectory tracking control of

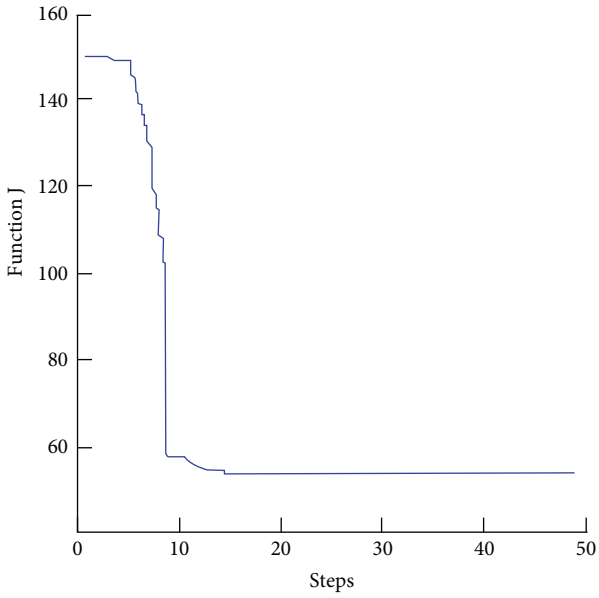

Figure 4: The curve of evaluation index function.

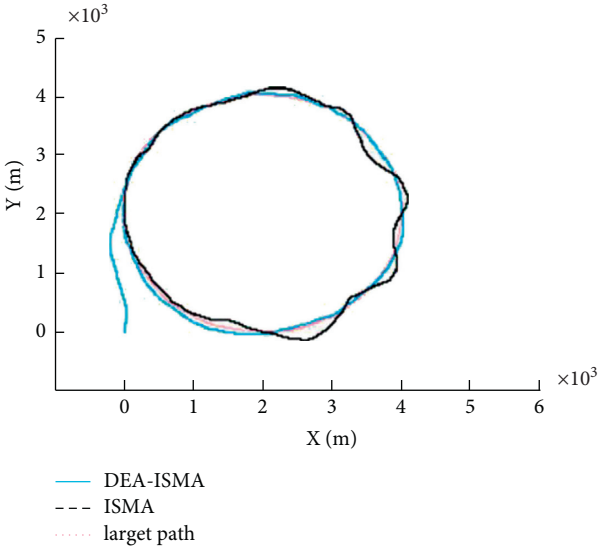

Figure 5: The curves of trajectory tracking.

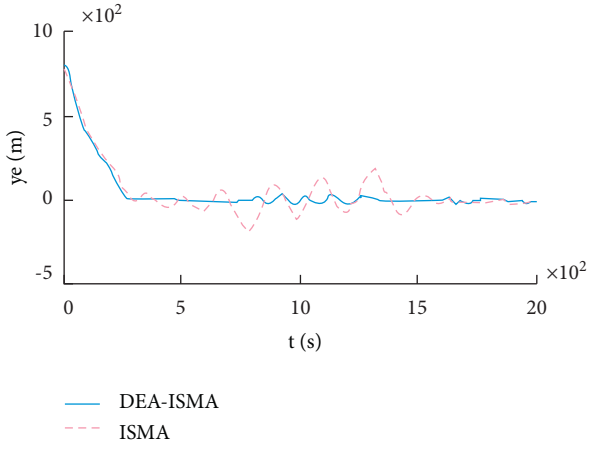

Figure 6: Error curve of lateral deviation y_e.

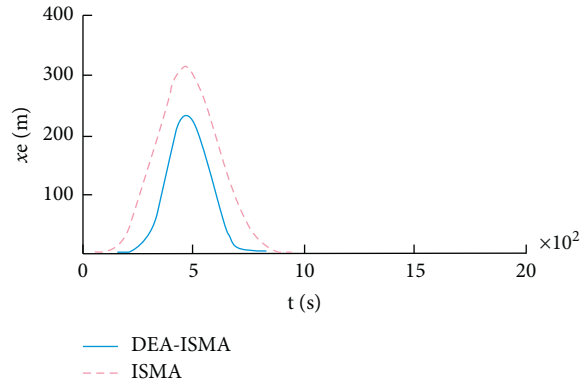

Figure 7: Error curve of longitudinal deviation x_e.

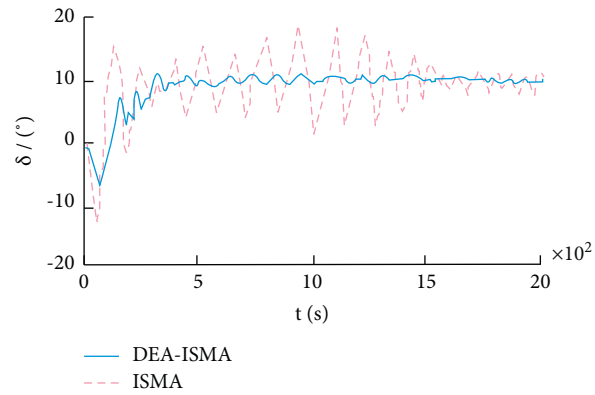

Figure 8: Change curve of control rudder angle δ.

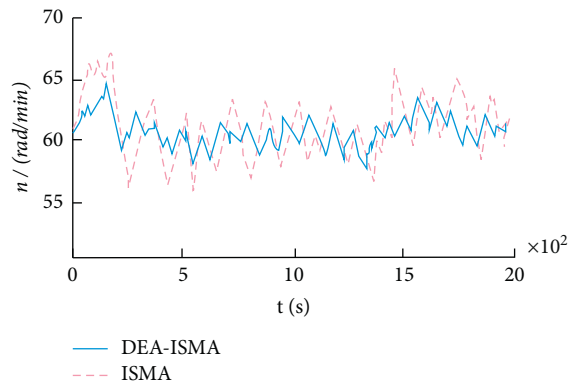

Figure 9: Speed change curve of main engine n.

the DEA-optimized ISMC controller is less than 240 m, while the maximum position deviation of the trajectory tracking control of the ISMC controller is 310 m; it is larger. It is obtained that the DEA-optimized ISMC controller can track faster than the ISMC controller, and the yaw distance in the control process is smaller, which will save energy in practical applications.

Figure 8 is the control rudder angle change curve. It is found from Figure 8 that the maximum rudder angle of the USV using the DEA-optimized ISMC controller is only 12°,

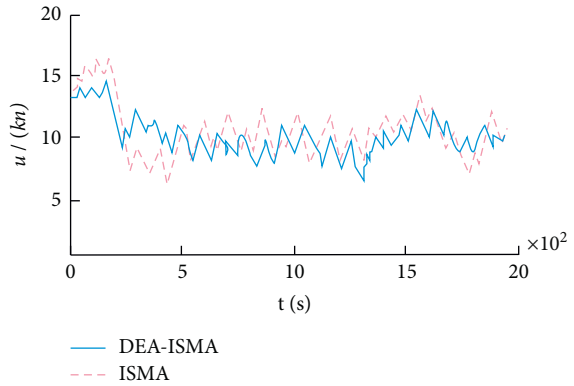

Figure 10: Speed curve of USV.

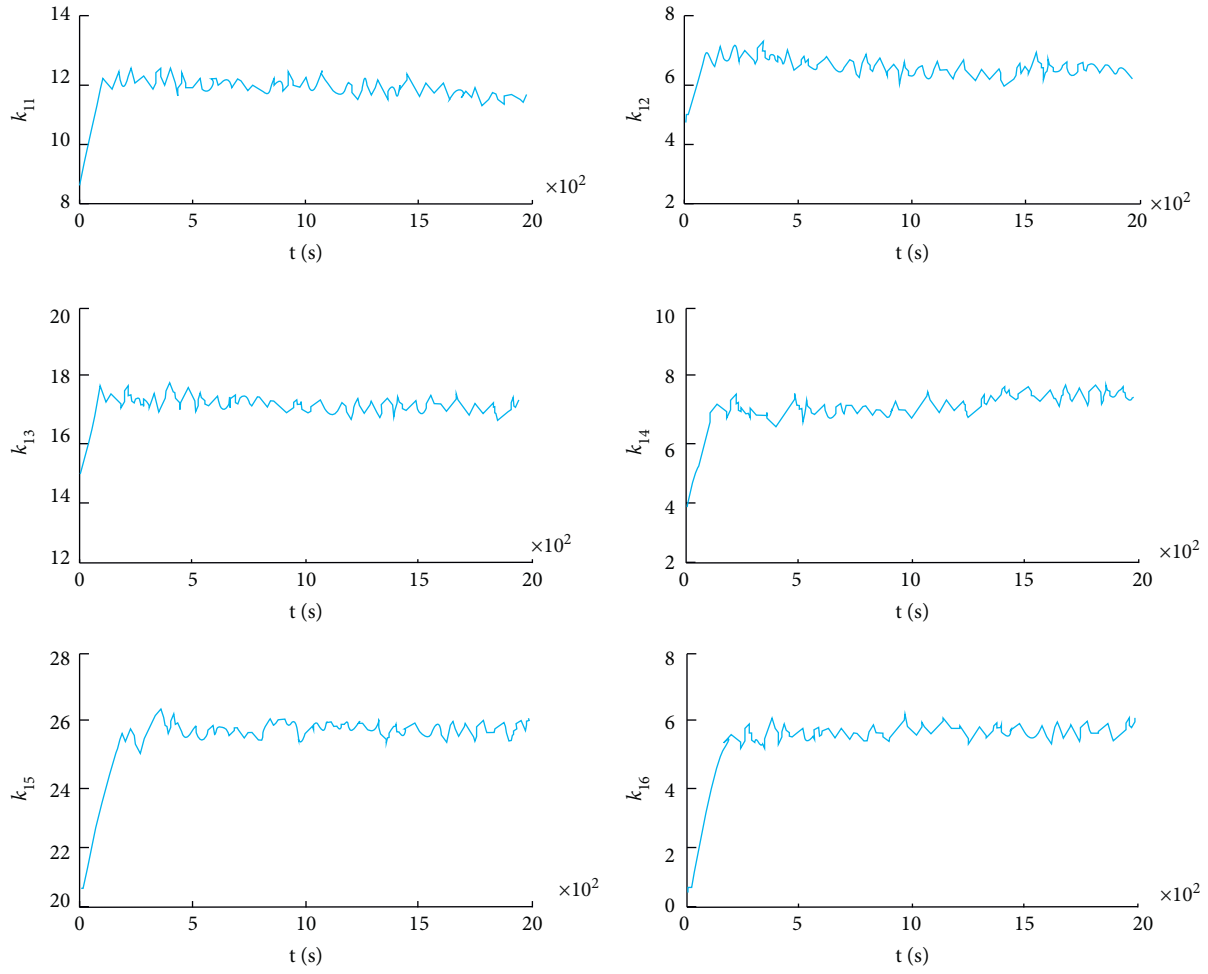

Figure 11: Change curve of parameters ($k_{11} \sim k_{16}$).

while using ISMC controller, it is about 18°; compared with the former, the applied rudder angle is increased by 50%. In addition, when the USV moves along a circular trajectory, the rudder angle output swing amplitude based on the DEA-optimized ISMC controller is less than 2°, while the rudder angle output swing amplitude based on the ISMC controller is about 5–6°, which is about 3 times that of the former. In engineering, the rudder angle swing amplitude is small and the wear and tear of the steering gear is small too, which is conducive to the working life of the steering gear. At this point, it is explained that the DEA-optimized ISMC controller is more suitable for the actual navigation of USV than the ISMC controller.

Figure 9 is the main engine speed change curve. It can be seen that after the introduction of the DEA optimization algorithm, the chattering changes are reduced

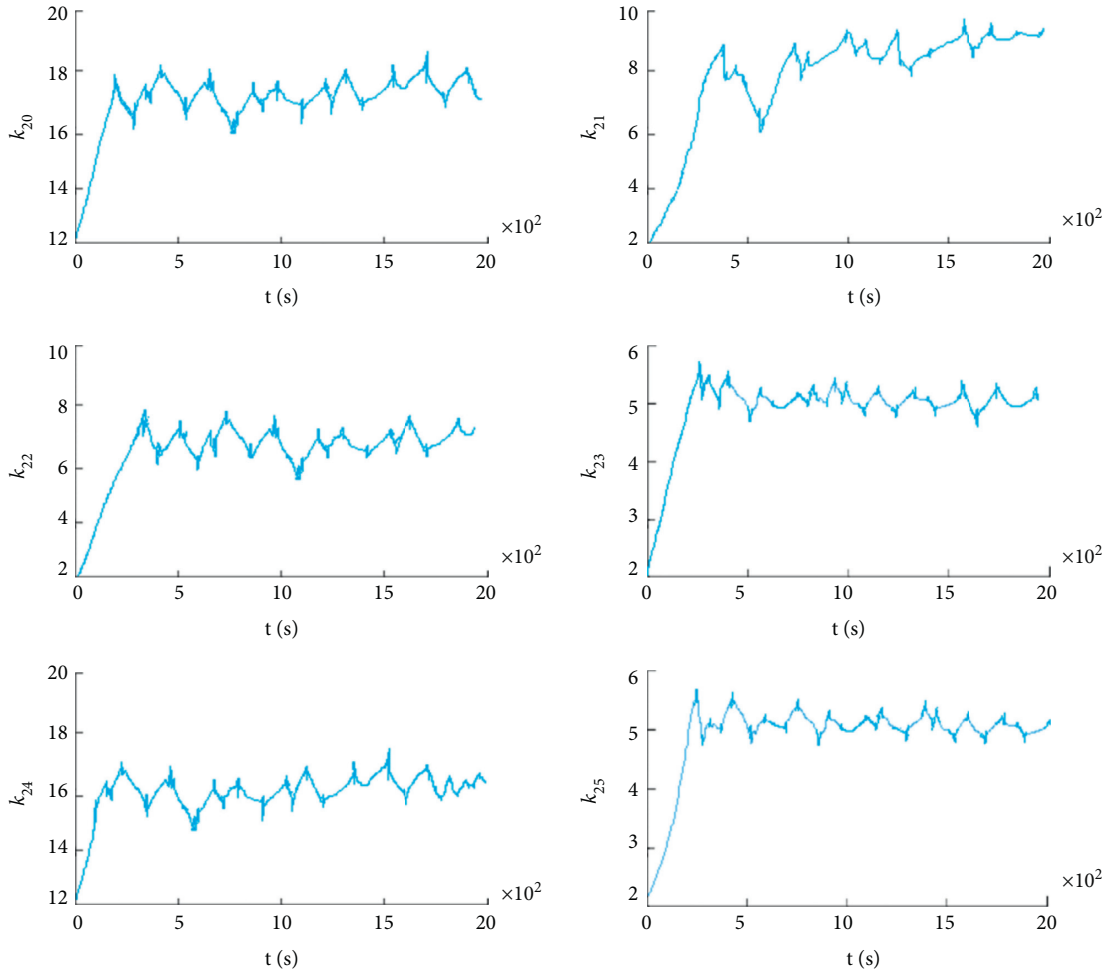

Figure 12: Change curve of parameters ($k_{20} \sim k_{25}$).

correspondingly, and the effect of reducing the rudder angle buffeting is obvious. From the ship speed curve shown in Figure 10, it can be seen that the ship speeds of the two methods basically track the target speed. Due to the interference of sea conditions such as wind current, the actual ship speed fluctuates up and down 15kn, and the fluctuation based on the DEA optimization algorithm is small.

Figures 11 and 12 are two types of parameters adjustment curve based on DEA optimization algorithm. The parameters ($k_{11} \sim k_{16}$) in design of controller for longitudinal deviation and the parameters ($k_{20} \sim k_{25}$) in design of controller for lateral deviation are learned in real time through the DEA optimization system, which play a role in the adjustment process of chattering of rudder angle and speed of main engine, so as to enhance the effect of controller self-adaptation.

Therefore, it can be concluded that the DEA-optimized ISMC controller has a better control effect than the ISMC controller. The former has better control performance; meanwhile, it is more in line with the actual USV project.

In addition, the demonstration of the influence of model parameters on the adaptability and robustness of the controller can be verified according to Figures 5 and 10. Referring to Figures 5 and 10, it can be seen that as the simulation progresses, the speed of the USV decreases with a maximum decrease of 50%; in this case, the designed optimized controller can still effectively track the predetermined circular trajectory. Therefore, it can be concluded that the designed control algorithm can still effectively track the preset trajectory when the speed parameters of the USV model change.

5. Conclusions

Taking into account that the driving source of Fossen model for trajectory tracking control is the three control variables of ship's longitudinal thrust, lateral thrust, and turning moment, it is difficult to apply to engineering practice. The DEA-optimized ISMC controller is designed to realize the trajectory tracking control for USVs via MMG model, and it is guaranteed through the theorem proposed that all signals in the system are consistent and eventually bounded.

Compared with ISMC controller, it is demonstrated that the proposed DEA-optimized ISMC controller has better control performance, smaller control chattering, and stronger robustness through computer simulation

experiment. Thus, the adaptive and robust performance of the designed DEA-optimized ISMC controller is verified.

Data Availability

The relevant data used for experimental verification have been included in the text.

Conflicts of Interest

The authors declare no conflicts of interest.

Authors' Contributions

All authors contributed equally.

Acknowledgments

This work was supported by the Basic Science (Natural Science) Research Project of Universities in Jiangsu Province under grants 21KJB580009 and 19KJD580001, the "Blue Project" for outstanding young backbone teacher talent project in Jiangsu Province in 2019 and 2021, the National Natural Science Foundation of China under grant no. 51909155, and the National Key R&D Program under grant no. 2019YFB1600602.

References

[1] M. Wondergem, E. Lefeber, K. Y. Pettersen, and H. Nijmeijer, "Output feedback tracking of ships," *IEEE Transactions on Control Systems Technology*, vol. 19, no. 2, pp. 442–448, 2011.

[2] Y. Fan, C. Li, G. Wang, G. Chen, and Y. Zhao, "Design and verification of heading tracking controller for unmanned surface craft," *Journal of Dalian Maritime University*, vol. 43, no. 1, pp. 1–7, 2017.

[3] X. He, H. Zhuang, D. Zhang, and Z. Qin, "Pulse neural network-based adaptive iterative learning control for uncertain robots," *Neural Computing & Applications*, vol. 23, no. 7/8, pp. 1885–1890, 2013.

[4] Y. Bai, Y. Zhao, and B. Qiu, "Design of efficient steering controller for unmanned surface vehicle," *China Navigation*, vol. 41, no. 4, pp. 68–71, 2018.

[5] A. S. K. Annamalai, R. Sutton, C. Yang, P. Culverhouse, and S. Sharma, "Robust adaptive control of an uninhabited surface vehicle," *Journal of Intelligent and Robotic Systems*, vol. 78, no. 2, pp. 319–338, 2015.

[6] S. Mobayen, H. Karami, and A. Fekih, "Adaptive nonsingular integral-type second order terminal sliding mode tracking controller for uncertain nonlinear systems," *International Journal of Control, Automation and Systems*, vol. 19, no. X, pp. 1–11, 2021.

[7] O. Mofid, S. Mobayen, and W.-K. Wong, "Adaptive terminal sliding mode control for attitude and position tracking control of q in the existence of external disturbance," *IEEE Access*, vol. 9, pp. 3428–3440, 2021.

[8] R. Wang, K. Miao, J. Sun, J. Li, and D. Chen, "Intelligent control algorithm for USV with input saturation based on RBF network compensation," *International Journal of Reasoning-Based Intelligent Systems*, vol. 11, no. 3, pp. 235–241, 2019.

[9] S. M. Esmaeilzadeh, M. Golestani, and S. Mobayen, "Chattering-free fault-tolerant attitude control with fast fixed-time convergence for flexible spacecraft," *International Journal of Control, Automation and Systems*, vol. 19, no. 2, pp. 767–776, 2021.

[10] C. Xiao, D. Zhou, Z. Liu, J. Zhang, and L. Wang, "Adaptive sliding mode track tracking control for underactuated unmanned vehicles," *Journal of National University of Defense Technology*, vol. 40, no. 3, pp. 127–134, 2018.

[11] L. Cheng, P. C. L. Chen, Z. J. Zou, and T. Li, "Adaptive NN–DSC control design for path following of underactuated surface vessels with input saturation," *Neurocomputing*, vol. 267, no. 12, pp. 466–474, 2017.

[12] W. Meng, G. Chen, F. Sun, and Y. Liu, "Nonlinear sliding mode trajectory tracking control of underdriven surface ships," *Journal of Harbin Engineering University*, vol. 33, no. 5, pp. 585–589, 2012.

[13] D. Xing and L. Zhang, "Sliding mode control of ship track tracking," *Ship*, vol. 22, no. 5, pp. 10–14, 2011.

[14] P. Zhang, Q. Chen, and T. Yang, "Trajectory tracking of autonomous ground vehicles with actuator dead zones," *International Journal of Computer Games Technology*, vol. 2021, Article ID 2914190, 2021.

[15] M. Fu, T. Wang, and C. Wang, "Barrier Lyapunov function-based adaptive control of an uncertain hovercraft with position and velocity constraints," *Mathematical Problems in Engineering*, vol. 2019, pp. 1–16, Article ID 1940784, 2019.

[16] Y. Tong, N. Sun, and Y. Fang, "Neuroadaptive control for complicated underactuated systems with simultaneous output and velocity constraints exerted on both actuated and unactuated states," *IEEE Transactions on Neural Networks and Learning Systems*, pp. 1–11, 2021.

[17] Z. Shen and X. Zhang, "Dynamic surface adaptive control of ship trajectory tracking based on nonlinear gain recursive sliding mode," *Acta Automatica Sinica*, vol. 44, no. 10, pp. 1833–1841, 2018.

[18] Z. Shen and C. Dai, "Reinforcement learning iterative sliding mode control for path tracking of underactuated ships," *Journal of Harbin Engineering University*, vol. 38, no. 5, pp. 697–704, 2017.

[19] R. Bu, Z. Liu, and T. Li, "Iterative sliding mode incremental feedback and its application in ship heading control," *Journal of Harbin Engineering University*, vol. 28, no. 3, pp. 268–272, 2007.

[20] H.-M. Jia, L.-J. Zhang, X.-Q. Cheng, X.-Q. Bian, Z.-P. Yan, and J.-J. Zhou, "Three-dimensional path following control for an underactuated UUV based on nonlinear iterative sliding mode," *Acta Automatica Sinica*, vol. 38, no. 2, pp. 308–314, 2012.

[21] Z. Shen, Y. Wang, H. Yu, and C. Guo, "Finite-time adaptive tracking control of marine vehicles with complex unknowns and input saturation," *Ocean Engineering*, vol. 198, Article ID 106980, 2020.

[22] Z. Shen and X. Zhang, "Iterative sliding mode heading control for self-inspired evaluation of sail-aided ships," *Journal of Harbin Engineering University*, vol. 38, no. 11, pp. 1727–1732, 2017.

[23] S. Zhao, W. Li, and W. Zhang, "Auto disturbance rejection control of ship track based on radial basis function neural network," *Journal of Shanghai Maritime University*, vol. 41, no. 4, pp. 20–24, 2020.

[24] H. Wang, D. Wang, and Z. Peng, "Adaptive dynamic surface control of multi-autonomous ship cooperative path tracking," *Control Theory & Applications*, vol. 30, no. 5, pp. 637–643, 2013.

[25] Z. Shen, Z. Jiang, and G. Wang, "Fuzzy adaptive iterative sliding mode control of sail-assisted ship motion," *Journal of Harbin Engineering University*, vol. 37, no. 5, pp. 634–639, 2016.

[26] K. Zhu, Z. Huang, and X. Wang, "Smart ship tracking control based on deep reinforcement learning," *Chinese Ship Research*, vol. 16, no. 1, pp. 105–113, 2021.

[27] R. Wang, D. Li, and K. Miao, "Optimized radial basis function neural network based intelligent control algorithm of unmanned surface vehicles," *Journal of Marine Science and Engineering*, vol. 8, no. 3, p. 210, 2020.

[28] R. Wang, Q. Li, S. Miao, K. Miao, and H. Deng, "Design of intelligent controller for ship motion with input saturation based on optimized radial basis function neural network," *Recent Patents on Mechanical Engineering*, vol. 14, no. 1, pp. 105–115, 2021.

[29] Y.-z. Jiang, L. Yu, L.-d. Yu, Y.-q. Chang, H.-k. Jia, and H.-n. Zhao, "Robot calibration based on modified differential evolution algorithm," *Optics and Precision Engineering*, vol. 29, no. 7, pp. 1580–1588, 2021.

[30] H. Deng, R. Wang, S. Hu, K. Miao, and Y. Yang, "Distributed genetic neural network optimal control of ship heading," *Journal of Shanghai Maritime University*, vol. 41, no. 4, pp. 15–19, 2020.

[31] C. Qi and X. Wang, "Non-singular fast terminal sliding mode and dynamic surface control trajectory tracking guidance law," *Journal of National University of Defense Technology*, vol. 42, no. 1, pp. 91–100, 2020.

[32] Z. Shen, *Adaptive Sliding Mode Control of Ship Motion*, Science Press, Beijing, China, 2019.